

# Radon and Thoron Exhalation Rate Measurements in Soil Samples Collected from the Vicinity of a Thermal Power Plant

Pankaj Kumar & Mukesh Kumar\*

Department of Physics, S.V. College, Aligarh, Uttar Pradesh 202 001, India

Received 20 June 2023; accepted 31 July 2023

Radon mass and thoron surface exhalation rate of soil samples collected from the surrounding area of Harduaganj thermal power plant (HTPP), Aligarh is measured using an active radon/thoron monitor (SMART RnDuo). The radon mass exhalation rate values range from  $27 \pm 1$  to  $100 \pm 3$   $\text{mBq kg}^{-1} \text{h}^{-1}$  with a mean value of  $63 \pm 17$   $\text{mBq kg}^{-1} \text{h}^{-1}$ . The thoron surface exhalation rate values vary from  $1.0 \pm 0.2$  to  $10 \pm 1$   $\text{kBq m}^{-2} \text{h}^{-1}$  with a mean value of  $5.7 \pm 2.2$   $\text{kBq m}^{-2} \text{h}^{-1}$ . The mean values of radon mass and thoron surface exhalation rate are found to be higher than the worldwide mean values.

**Keywords:** Soil samples; SMART RnDuo; Exhalation rates

## 1 Introduction

Radon exhalation measurements from soil and building material samples are important to know the radon risk to human populations<sup>1</sup>. Radon and its progeny are the significant contributors to the average dose from natural background sources of radiation and constitute approximately half of the total dose to the general population. Epidemiologic studies in Europe and other case-control investigations in China and North America show that exposure to radon increases the risk of lung cancer<sup>2-4</sup>. Radon, a radioactive inert gas, escapes from grain as a result of recoil and if the recoil terminates in open pore space, radon becomes available to migrate<sup>5</sup>. Radon which is available in the interstitial space may be transported to the surface by diffusion and advective flow and released into the atmosphere, referred to as radon exhalation<sup>6</sup>. Diffusion, which is usually the dominant transport mechanism, is caused by the radon concentration gradient

While advection takes place if there is a pressure difference between the air of the pore space and the ground surface<sup>7</sup>. The infiltration of radon gas from soil has been identified as one of the main mechanisms influencing indoor radon levels in buildings. It is reported that more than 90% of the contribution to indoor radon comes from the ground and surrounding soil of a building<sup>8</sup>. Under normal conditions, thoron concentrations in soil gas are roughly comparable to

the radon concentrations because of the similar production rates in rocks and soils and their similar behavior in the ground<sup>9</sup>. However, high thoron entry rates from the ground are rarely encountered. Because of its short half-life (55 sec), most of the thoron decays before reaching the surface.

Radon and thoron gases are members of the  $^{238}\text{U}$  and  $^{232}\text{Th}$  decay series, respectively, widely distributed in the earth's crust. Since both gases are members of different decay chains, their concentrations in the atmosphere depend on the  $^{238}\text{U}$  and  $^{232}\text{Th}$  contents, respectively, in local soil and building materials. Various factors such as radium content, soil morphology, grain size, porosity, and radon flux density directly influence radon exhalation dynamics while meteorological parameters like temperature, pressure, and humidity indirectly affect the process of exhalation in soil<sup>10,11</sup>.

In the present study radon mass ( $J_m$ ) and thoron surface ( $J_s$ ) exhalation rates in soil samples collected from the surrounding area of about 90  $\text{km}^2$  around HTPP situated are measured using a continuous radon monitor (SMART RnDuo)<sup>12</sup>.

## 2 Material and Methods

The installed capacity of HTPP ( $28^\circ 01' 03'' \text{N}$   $78^\circ 07' 48'' \text{E}$ ) is 665 MW having seven generation units. Longitudes and latitudes of the study area around HTPP vary from  $78.0925^\circ$  to  $78.1810^\circ$  and  $27.9722^\circ$  to  $28.0510^\circ$ , respectively. The soil of this area is sandy loam soil with brown or radish color.

\*Corresponding author: (E-mail: mksvc@rediffmail.com)

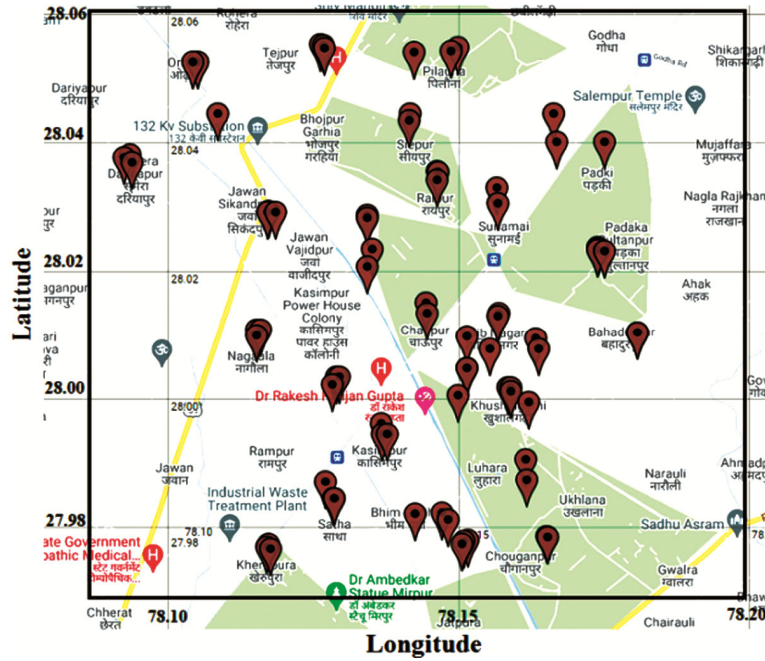


Fig. 1 — Samples locations around HTPP, Aligarh.

A total of 75 samples were collected from twenty-five villages. The locations of the soil samples taken for exhalation rate studies are shown in Fig. 1.

Technical specifications and experimental procedures for the measurement of  $J_m$  and  $J_S$  are discussed in detail elsewhere<sup>13</sup>. The SMART RnDuo is operated in diffusion mode with 1-hour cycles for the measurement of  $J_m$ .

The radon concentration  $C_{Rn}(t)$  buildup in the accumulation chamber at time  $t$  after closing the chamber can be calculated as per the following relation<sup>13</sup>

$$C_{Rn}(t) = \frac{J_m M}{V \lambda_e} [1 - e^{-\lambda_e t}] + C_{Rn}(0) e^{-\lambda_e t} \quad \dots(1)$$

where  $C_{Rn}(0)$  represents the initial radon concentration ( $Bq\ m^{-3}$ ) present in the chamber volume at  $t = 0$ ,  $J_m$  is the radon mass exhalation rate, measured in  $Bqkg^{-1}h^{-1}$ ,  $M$  is the total mass of the dry sample, measured in kg,  $V$  is the residual air volume in the measurement system, which includes the detector volume of 150cc, the residual air volume of the exhalation chamber, and porous volume of the sample measured in  $m^3$ ,  $\lambda_e$  is the effective decay constant, which is the sum of the leak rate (if any) and the radon decay constant. The measurement time,  $t$  is measured in hours. If measurement time is limited to 12 hours, a linear approximation can be used and the Eq. (1) can be written as:

$$C_{Rn}(t) = \frac{J_m M}{V} t + C_{Rn}(0) \quad \dots(2)$$



Fig. 2 — Set up for the measurement of  $J_m$ .

By performing a least-square fitting of the data to Equation (2) mentioned above, the value of  $J_m$  can be determined using the slope obtained from the fitting, along with the mass ( $M$ ) of the sample and the residual air volume ( $V$ ) of the setup.

However, for the measurement of  $J_S$ , the SMART RnDuo is operated in a flow mode with 15-minute cycles. To calculate the thoron surface exhalation  $J_S$  ( $Bqm^{-2}h^{-1}$ ) rate of the sample, the following Equation (3) is used<sup>13</sup>

$$J_S = \frac{C_{Th} V \lambda}{A} \quad \dots(3)$$

where  $C_{Th}$  is the equilibrium thoron concentration ( $Bqm^{-3}$ ).  $V$  is the residual air volume of the setup ( $m^3$ ).  $A$  is the surface area of the sample ( $m^2$ ), and  $\lambda$  is the decay constant ( $44.87h^{-1}$ ) for thoron.

The accuracy in the estimation of  $J_m$  and  $J_S$  with this device is under 10% and 20% respectively. Figs 2 & 3 show the SMART RnDuo setup for the measurement of  $J_m$  and  $J_S$ , respectively.

Fig. 3 — Set up for the measurement of  $J_S$ .

### 3 Results and Discussion

Global Positioning System (GPS) coordinates of soil samples and experimentally determined values of  $J_m$  and  $J_S$  along with their statistical values of parameters are given in Table 1.

The measured values of  $J_m$  are found to vary from  $27 \pm 1$  to  $100 \pm 3$   $\text{mBq kg}^{-1} \text{h}^{-1}$ . The median and the mean values with one slandered deviation are  $60 \text{ mBq kg}^{-1} \text{h}^{-1}$  and  $63 \pm 17 \text{ mBq kg}^{-1} \text{h}^{-1}$ , respectively. The observed wide variation in  $J_m$  may be due to the

Table 1 — GPS coordinates,  $J_m$ , and  $J_S$  of soil samples collected from the surrounding region of HTPP

Village	Sample code	GPS coordinates		$J_m(\text{mBqkg}^{-1}\text{h}^{-1})$	$J_S(\text{kBqm}^{-2}\text{h}^{-1})$
		Latitude (degree)	Longitude (degree)		
Sumera	H01	28.0338	78.0936	46±2	5.6±0.4
	H02	28.0326	78.0939	36±4	5.3±0.4
	H03	28.0333	78.0925	51±1	3.5±0.4
Nagaula	H04	28.0056	78.1154	74±2	5.8±0.5
	H05	28.0066	78.1153	62±2	6.6±0.6
	H06	28.0065	78.1161	80±2	7.3±0.6
Rampur	H07	27.9991	78.1291	86±4	7.4±0.5
	H08	27.9991	78.1297	58±1	4.9±0.5
	H09	27.9979	78.1284	66±2	3.4±0.4
Kheraupura	H10	27.9731	78.1174	61±1	3.5±0.4
	H11	27.9722	78.1178	38±1	2.7±0.4
	H12	27.9726	78.1170	54±2	8.4±0.5
Satha	H13	27.9801	78.1285	48±6	8.3±0.6
	H14	27.9801	78.1287	79±2	6.4±0.5
	H15	27.9828	78.1272	51±2	6.7±0.6
Jarauthi	H16	27.9737	78.1518	71±3	3.8±0.4
	H17	27.9735	78.1510	59±2	2.4±0.3
	H18	27.9730	78.1508	53±4	1.3±0.2
Bheemgarhi	H19	27.9768	78.1483	68±6	3.1±0.3
	H20	27.9779	78.1473	90±3	1.4±0.2
	H21	27.9778	78.1426	96±11	1.3±0.2
Kaasimpur	H22	27.9830	78.1619	51±2	1.0±0.2
	H23	27.9862	78.1617	63±2	1.3±0.2
	H24	27.9952	78.1622	89±7	1.1±0.2
	H25	27.9902	78.1370	90±4	3.5±0.3
Luhara	H26	27.9902	78.1378	100±3	3.0±0.3
	H27	27.9918	78.1369	97±3	1.3±0.3
	H28	28.0005	78.1516	94±2	4.3±0.4
Bhootpura	H29	28.0005	78.1516	27±1	5.2±0.4
	H30	28.0055	78.1516	41±4	5.8±0.5
	H31	28.0052	78.1634	42 ±2	6.6±0.5
Kherakhurd	H32	28.0035	78.1639	42±3	4.3±0.4
	H33	28.0061	78.1810	42±3	6.6±0.5
	H34	28.0192	78.1742	91±2	7.2±0.5
Gopalpur	H35	28.0194	78.1741	58±2	4.9±0.4
	H36	28.0189	78.1740	60±1	5.1±0.4
	H37	28.0091	78.1570	77±1	5.3±0.5
Talibnagar	H38	28.0086	78.1569	60±2	4.7±0.4
	H39	28.0035	78.1555	64±2	6.6±0.6

(Contd.)

Table 1 — GPS coordinates,  $J_m$ , and  $J_S$  of soil samples collected from the surrounding region of HTPP (Contd.)

Village	Sample code	GPS coordinates		$J_m(\text{mBqkg}^{-1}\text{h}^{-1})$	$J_S(\text{kBqm}^{-2}\text{h}^{-1})$
		Latitude (degree)	Longitude (degree)		
Chauganpur	H40	27.9742	78.1653	83±3	5.7±0.5
	H41	27.9741	78.1655	51±2	7.0±0.5
	H42	28.0061	78.1810	72±1	9.4±0.6
Chaupur	H43	27.9962	78.1501	56±2	5.3±0.5
	H44	28.0107	78.1445	48±3	9.2±0.6
	H45	28.0091	78.1447	77±5	6.8±0.6
	H46	28.0164	78.1345	58±2	6.6±0.7
Sunamai	H47	28.0262	78.1569	60±2	5.4±0.6
	H48	28.0286	78.1568	46±2	6.7±0.6
Padki	H49	28.0358	78.1753	63±2	4.4±0.6
	H50	28.0188	78.1752	67±1	6.7±0.6
	H51	28.0357	78.1670	72±2	7.8±0.6
Pilauna	H52	28.0504	78.1500	81±2	7.8±0.6
	H53	28.0499	78.1489	98±2	10±1
	H54	28.0402	78.1666	59±1	8.9±0.7
	H55	27.9969	78.1591	60±2	7.7±0.6
Khushaalgarhi	H56	27.9975	78.1587	47±2	5.1±0.5
	H57	27.9974	78.1592	77±2	8.5±0.6
Jawan Vajidpur	H58	28.0244	78.1345	47±1	5.2±.5
	H59	28.0191	78.1352	56±1	7.1±0.6
	H60	28.0240	78.1345	66±1	7.3±0.6
Raipur	H61	28.0311	78.1466	56±2	6.6±0.6
	H62	28.0312	78.1465	69±2	7.5±0.6
	H63	28.0299	78.1464	46±2	6.2±0.5
Siepur	H64	28.0401	78.1418	50±2	7.2±0.5
	H65	28.0497	78.1425	52±1	8.4±0.6
	H66	28.0391	78.1417	59±2	8.0±0.6
Tejpur	H67	28.0507	78.1268	84±3	9.2±0.6
	H68	28.0510	78.1264	68±2	7.6±0.6
	H69	28.0503	78.1270	73±2	8.6±0.6
Jawan Sikandpur	H70	28.0250	78.1175	49±1	5.3±0.5
	H71	28.0249	78.1172	47±2	5.4±0.5
	H72	28.0249	78.1186	52±2	5.7±0.5
Auhriya	H73	28.0482	78.1052	52±1	8.8±0.5
	H74	28.0482	78.1044	42±2	4.1±0.4
	H75	28.0401	78.1086	63±2	5.5±0.5
	Minimum			27±1	1.0±0.2
	Maximum			100±3	10±1
	Median			60	5.8
	Average ± SD			63±17	5.7±2.2
	Excess kurtosis			-0.5	-0.4
	Skewness			0.5	-0.4

radon emanation factor, and porosity of soil samples<sup>14</sup>. Sample H 26 of village Luhara has a maximum value of  $J_m$  ( $100\pm3 \text{ mBq kg}^{-1} \text{ h}^{-1}$ ) while the sample H 29 ( $27\pm1 \text{ mBq kg}^{-1} \text{ h}^{-1}$ ) of village Bhootpura has a minimum value of  $J_m$  as shown in Table 1.

The excess kurtosis is less than zero (-0.5), showing platykurtic distribution. The skewness (0.5) is between -5 and +5, indicating that the distribution

is approximately symmetric. The values of  $J_S$  vary from  $1.0 \pm 0.2$  to  $10\pm1 \text{ kBq m}^{-2}\text{h}^{-1}$  with a mean value of  $5.7 \pm 2.2 \text{ kBq m}^{-2}\text{h}^{-1}$ . The median value is  $5.8 \text{ kBq m}^{-2}\text{h}^{-1}$ . In the soil sample (H 53) collected from village Pilonathe value of  $J_S$  is found to be highest and is  $10\pm1 \text{ kBq m}^{-2}\text{h}^{-1}$ . The lowest level is  $1.0 \pm 0.2 \text{ kBq m}^{-2}\text{h}^{-1}$  found in a soil sample (H 22) of village Kasimpur (Table 1). The value of excess kurtosis is found to be -0.4 which is less than zero, showing that

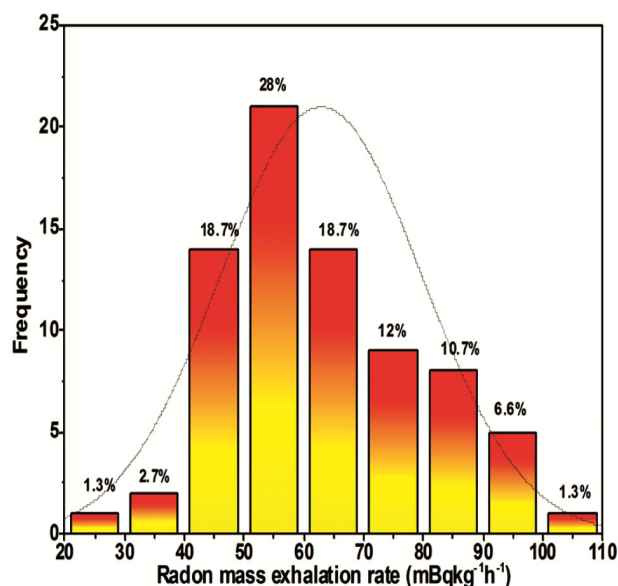


Fig. 4 — Distribution curve of  $J_m$  in the surrounding region of HTPP, Aligarh.

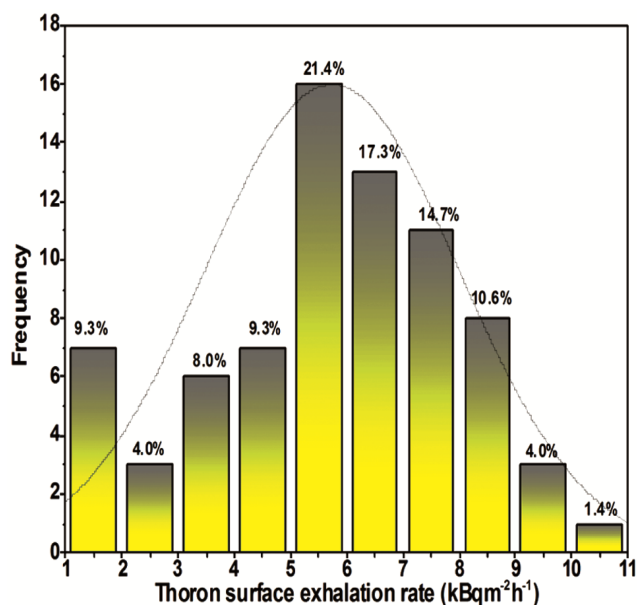


Fig. 5 — Distribution curve of  $J_s$  in the surrounding region of HTPP, Aligarh.

the nature of distributions is platykurtic. The value of skewness (-0.4) shows that the distribution is approximately symmetric.

The frequency distributions of  $J_m$  and  $J_s$  are given in Figs. 4 & 5, respectively. Notably, about 69% of the samples have a value of  $J_m$ , and about 79% of the samples have a value of  $J_s$  higher than worldwide mean values of  $57 \text{ mBqkg}^{-1} \text{ h}^{-1}$  and  $3.6 \text{ kBq m}^{-2} \text{ h}^{-1}$  for radon mass and thoron surface exhalation rate, respectively<sup>15</sup>.

## Conclusions

The average value ( $63 \text{ mBq kg}^{-1} \text{ h}^{-1}$ ) of  $J_m$  in the soil of the surrounding region of HTPP, Aligarh is found to be higher than the worldwide mean value of  $57 \text{ mBqkg}^{-1} \text{ h}^{-1}$ . The average value of  $J_s$  ( $5.7 \text{ kBqm}^{-2} \text{ h}^{-1}$ ) is also found to be higher than the worldwide mean value of  $3.6 \text{ kBq m}^{-2} \text{ h}^{-1}$ . The distribution of  $J_m$  and  $J_s$  in the study area is found to be approximately symmetric.

## Acknowledgment

The authors are thankful to the Board of Research in Nuclear Science (BRNS), Department of Atomic Energy, Government of India (Project Ref. No.: 2013/36/59-BRNS/2468) for providing financial assistance to carry out this study.

## References

- Nazaroff WW & Nero AV, *Radon and its decay product in indoor*, (John Wiley and Sons, New York), 1988.
- Lubin J H, Wang Z Y, Boice J D, Xu Z Y, Bolt J W, De Wang L & Kleinerman A R, *Int J Cancer*, 109 (2004) 132.
- Kerwski D, Lubin J H, Zielinski J M, Alavanja M, Catalan V S, Field R W, Klotz J B, Letourneau E G, Schoenberg J B, Steck D J, Stolwijk J N, Weinberg C & Wilcox H B, *Epidemiology*, 16 (2005) 137.
- Darby S C, Hill D, Deo H, Auvinen A, Barros-Dios J M, Baysson H, Bochicchio F, Falk R, Farchi S, Figueiras A, Hakama M, Heid I, Hunter N, Kreienbrock L, Kreuzer M, Lagarde F, Makelainen I, Muirhead C, Oberaigner W, Pershagen G, Ruosteenoja E, Rosario AS, Tirmarche M, Tomasek L, Whitely E, Wichmann H E & Doll R, *Scand J Work Environ Health*, 32 (2006) 1.
- UNSCEAR, United Nations Scientific Committee on the Effects of Atomic Radiation: Sources and effects ionizing radiation: Report to the General Assembly with Scientific Annexes, Annex B: Exposure from natural sources of radiation, United Nations, New York, 2000.
- Ishimori Y, Lange K & Martin P, Technical reports series no. 474, International Atomic energy Agency, Vienna, 2013.
- Sun K, Guo Q & Zhuo W, *J Nucl Sci Technol*, 41 (2004) 86.
- Nero A V, Gadgil A J, Nazaroff W W & Revzan K L, Technical Report, U.S. Department of Energy, Office of Health and Environmental Research Washington, D C, 20545 (1990).
- Hutter A R, *Environ Int J*, 22 (1996) 455.
- Khan M S, Srivastava D S & Azam A, *Environ Earth Sci*, 67 (2012) 1363.
- Sharma S, Kumar A, Mehra R & Mishra R, *J Soils Sediments*, 19 (2019) 1441.
- Gaware J J, Sahoo B K, Sapra B K & Mayya Y S, *BARC News Lett*, 318 (2011) 45.
- Sahoo B K, Sapra B K, Kanse S D, Gaware J J & Mayya Y S, *Radiat Meas*, 58 (2013) 52.
- Sahoo B K, Agarwal T K, Gaware J J & Sapra B K, *J Radioanal Nucl Chem*, 302 (2014) 1417.
- Prajith R, Rout R P, Kumbhar D, Mishra R, Sahoo B K & Sapra B K, *Environ Earth Sci*, 78 (2019) 35.